

Temperature and Vibration Insensitive Fiber-Optic Current Sensor

K. Bohnert, P. Gabus, and H. Brändle

ABB Corporate Research Ltd, CH-5405 Baden-Dättwil, Switzerland
Phone: +41 56 486 8044, Fax: +41 56 493 7068, E-mail: klaus.bohnert@ch.abb.com

ABSTRACT

We present a robust, temperature and vibration insensitive fiber-optic current sensor. The sensor has been integrated into a high-voltage circuit breaker. One year field experience has been gained in two substations of the Italian railways.

1. INTRODUCTION

Optical fiber current sensors for the electric power industry have been under investigation for about two decades. In the past, a number of technical shortcomings such as unacceptable sensitivity to temperature and vibration as well as concerns about their long-term reliability have contributed to prevent extended commercial use. The sensors should be accurate within $\pm 0.2\%$ for temperatures between -40 and $+85^\circ\text{C}$. In the following we report a sensor which, we believe, meets the important performance requirements and describe some experience we have gained in the field.

2. SENSOR CONFIGURATION

Two configurations of the sensor have been investigated and compared. In the Sagnac configuration^{1,2} (Fig. 1, top) the magnetic field of the current induces, as a result of the Faraday effect, a differential optical phase shift between two circular polarizations of the same handedness counter-propagating in a coil of sensing fiber. The phase shift is given by $\Delta\theta_S = 2 V N I$, where V is the Verdet constant of the fused silica fiber, N is number of fiber loops, and I is the current. The circular polarizations are generated from linear polarizations prior to entering the coil by means of two short sections of elliptical-core fiber acting as quarter-wave retarders. Upon leaving the coil the circular polarizations are converted back to linear. An appropriately adapted optoelectronics module of a commercial fiber gyroscope provides the light source (820 nm) and is used to detect the current-induced optical phase shift between the optical waves. Gyroscopes with open-loop as well as with closed loop detection circuits were employed. Elliptical-core fibers serve to transmit the linear polarizations between gyro module and coil.

In the reflection configuration^{3,5} (Fig. 1, bottom), left and right circular polarizations are co-propagating in the coil. They are produced by a single fiber $\lambda/4$ retarder from two orthogonal linear polarizations transmitted by the elliptical-core fiber lead. The two circular waves are reflected at the coil end (with swapped polarizations), converted back to orthogonal linear polarizations at the retarder, and finally brought to interference in the fiber polarizer of the gyroscope module. Here, the current-induced phase shift is given by $\Delta\theta_R = 4 V N I$. The sensor allows to measure ac as well as dc currents.

Fig. 2 illustrates the preparation and packaging of the sensing fiber coil. The bare sensing fiber (low-bi fiber with $80\ \mu\text{m}$ outer diameter) with the retarders is housed and has been thermally annealed⁶ in a coiled capillary of fused silica. The residual birefringence after annealing is typically between 2 and 6 degrees and is independent of temperature. Coils with up to 15 fiber loops and with diameters of 137 and 117 mm were investigated. The coiled capillary is embedded in a polymer inside a robust ring-shaped housing. Deterioration of the sensor response due to stress-induced birefringence is thus avoided in a simple manner over the full temperature range of operation (-40 to 85°C). Furthermore, we make use of the small temperature dependence of the elliptical-core fiber retarder(s) to compensate the intrinsic temperature dependence of the magneto-optic effect (i.e. of the Verdet constant, $0.7 \times 10^{-4}/^\circ\text{C}$). If the retardation, ϕ , is chosen as 75° rather than 90° , the variation in scale factor^{3,5} as a result of the temperature dependence of the retarder(s) ($\delta\phi/\delta T = -0.0153/^\circ\text{C}$) cancels the influence of the temperature variation of the Verdet constant (Fig. 3). In the Sagnac configuration the compensation requires that the fast axes of the retarders are aligned at a defined angle to each other. We have developed an efficient procedure to prepare the retarders, which allows to accurately fix their length and retardation and which does not require splicing with 45° core orientation. First, the sensing fiber is spliced to a section of elliptical-core fiber. Next, a 45° twist is introduced over a fiber section with a length of several centimeters or more which includes the splice. The elliptical-core fiber is then heated in the arc of the fusion splicer at a location which is separated from the end of the sensing fiber by the desired retarder length. The twist relaxes resulting in a permanent 45° offset in the core orientation at the location where the fiber was heated.

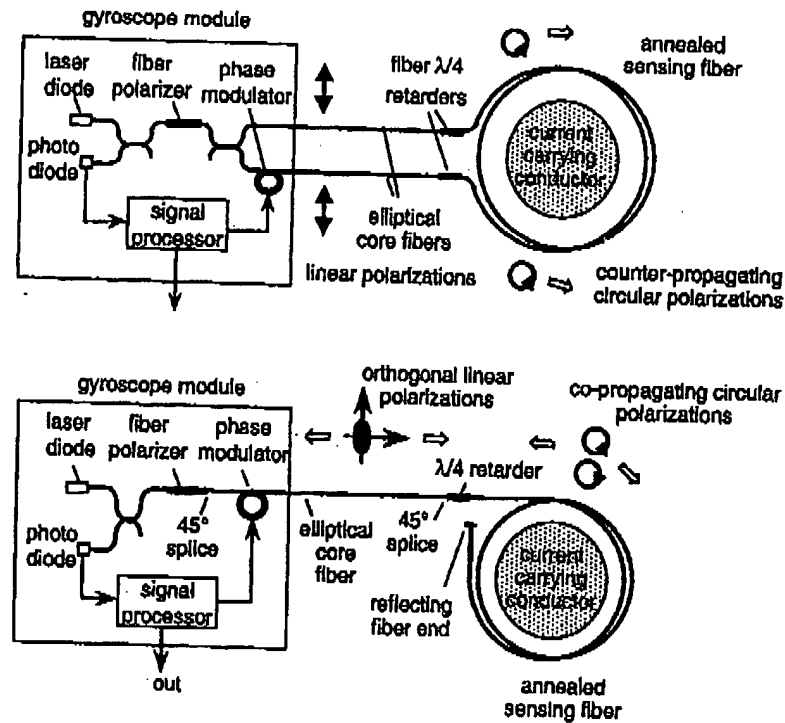


Figure 1. Optical fiber current sensor: Sagnac configuration (top), reflection configuration (bottom).

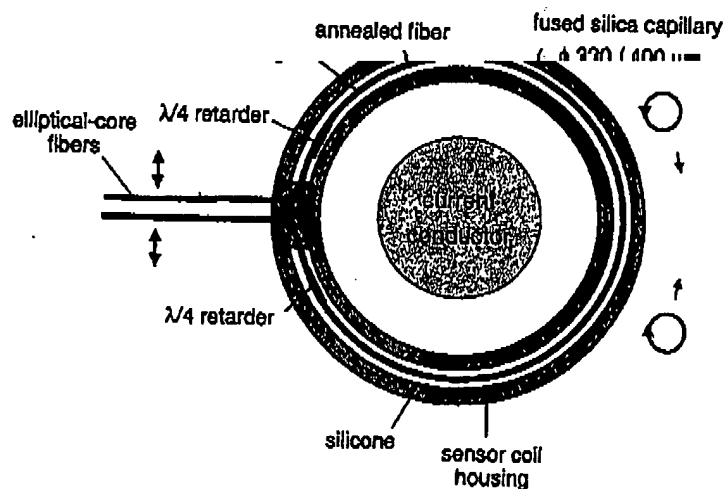


Figure 2. The bare sensing fiber is housed and thermally annealed in a capillary of fused silica. The coiled capillary is embedded in a polymer inside a robust coil housing. For clarity only one fiber loop is shown.

3. EXPERIMENTAL RESULTS AND DISCUSSION

Fig. 4 shows the sensor signal as a function of the coil temperature (four fiber loops). Here, the residual temperature dependence is $0.23 \times 10^{-4} / ^\circ\text{C}$ over the temperature range of interest and is sufficiently small to meet the requirements for applications in the electric power industry. With four fiber loops the minimum detectable current is 85mA rms/ $\sqrt{\text{Hz}}$ at 50 Hz (Sagnac configuration), which is, for the present optical power level, close to the theoretical limit. The maximum detectable current is 27 kA rms for the open loop and 63 kA rms for the closed loop detection circuit. A major advantage of the reflection configuration is that mechanical perturbations of the fiber coil and the fiber lead essentially do not show up in the sensor output. The relatively small

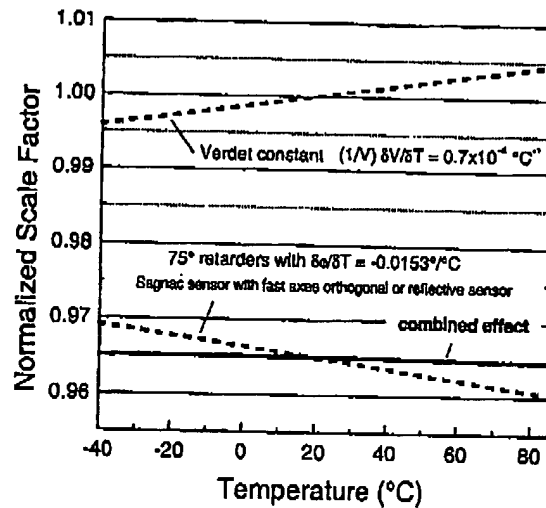


Figure 3. Inherent temperature compensation: the properly combined contributions of Verdet constant and retarder(s) to the temperature dependence of the scale factor result in a temperature insensitive sensing coil.

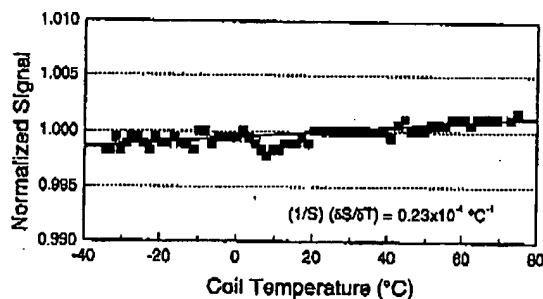


Figure 4. Sensor signal as a function of temperature of sensing fiber coil.

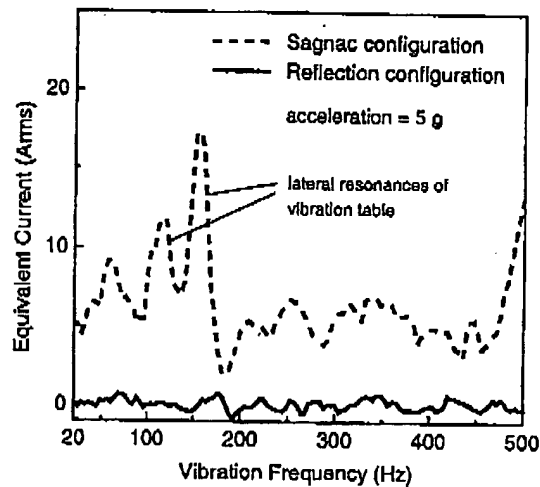


Figure 5. Vibration-induced signal (coil vibration) in terms of equivalent current as a function of vibration frequency for the Sagnac and reflective sensor configurations, respectively. The acceleration is 5 g.

perturbation of the differential phase of the co-propagating optical waves, as a result of time-varying mechanical disturbances, is largely canceled on their return trip, since the returning waves have exchanged their states of polarization. In the Sagnac configuration, on the other hand, the disturbance of the differential optical phase is significantly larger. In order to evaluate the sensor performance under mechanical perturbations, the sensor coil and fiber cable were subjected to shocks of 100 g (half sine wave with 6 ms duration) and harmonic accelerations of up to 10 g and varying frequency. The outstanding performance of the reflection configuration is seen in Fig. 5, which compares for both schemes the sensitivity to vibration of the fiber coil in the range between 20 and 500 Hz at an acceleration of 5 g. Further investigations focused on the long-term stability of the sensor, effects of magnetic stray fields and high levels of humidity.

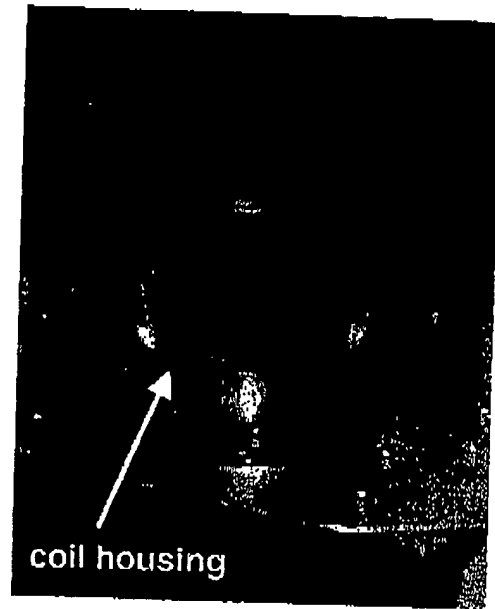
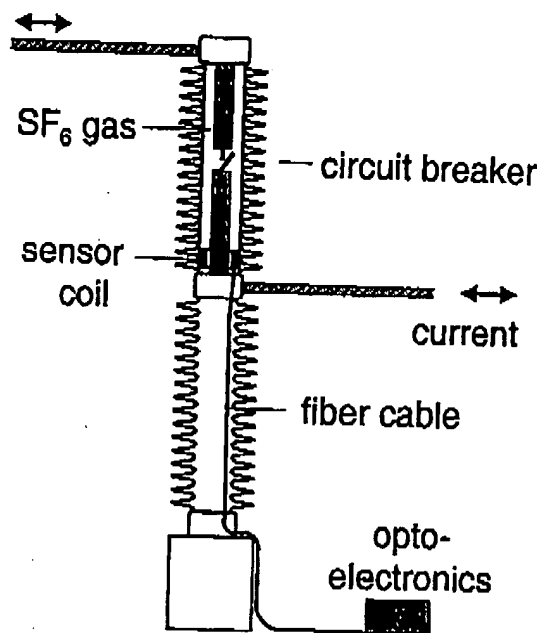


Figure 6. Integration of sensor coil into 170 kV high-voltage circuit breaker. The photograph (right) shows the coil housing at the bottom end of the breaker mechanism.

4. FIELD EXPERIENCE

In a first application several sensors have been integrated in 170 kV high-voltage circuit breakers for subsequent field tests. The fiber coil is within the pressurized SF_6 gas atmosphere of the breaker and encompasses the bottom end of the breaker mechanism (Fig. 6). The fiber cable (here with a length of 30 m) leaves the breaker through a gas-tight feed-through and continues to the detection circuit which is outside the breaker. Furthermore, a number of sensors for DC currents have been installed in two substations of the Italian railways. Eight sensors were reexamined after one year of service. Within the experimental uncertainty ($\pm 0.3\%$) the scale factors of seven sensors were found to be unchanged. (For the eighth sensor an electronics problem was noticed).

5. CONCLUSIONS

The experimental results show that the fundamental problems which have limited the performance of fiber-optic current sensors in the past have been essentially resolved. Next steps towards commercial use will include optimizing of the manufacturing procedures, adaptation of the sensor to different applications, and further demonstration of the sensor performance in the field.

REFERENCES

1. P. A. Nicati and P. Robert, "Stabilized current sensor using a Sagnac interferometer", *J. Phys. E*, vol. 21, 791-796, 1988.
2. G. Frosio, K. Hug, and R. Dändliker, "All-fiber Sagnac current sensor", in *Opto '92* (ESI Publications, Paris 1992), 560-564.
3. G. Frosio, *Ph.D. Thesis* 1992, University of Neuchâtel, Switzerland.
4. G. Frosio and R. Dändliker, "Reciprocal reflection interferometer for a fiber-optic Faraday current sensor", *Appl. Opt.*, vol. 33(25), 6111-6122, 1994.
5. J. Blake, P. Tantaswadi, and R.T. de Carvalho, "In-line Sagnac interferometer current sensor", *IEEE Trans. Power Deliver*, vol. 11(1), 116-121, 1996.
6. D. Tang, A. H. Rose, G. W. Day, and S. M. Etzel, "Annealing of linear birefringence in single-mode fiber coils: applications to optical fiber current sensors", *J. Lightw. Technol.*, vol. 9(8), 1031-1037, 1991.